

Weak and strong typicality in quantum systems

Lea F. Santos,¹ Anatoli Polkovnikov,² and Marcos Rigol³

¹*Department of Physics, Yeshiva University, New York, NY 10016, USA*

²*Department of Physics, Boston University, Boston, MA 02215, USA*

³*Department of Physics, Georgetown University, Washington, DC 20057, USA*

We study the properties of mixed states obtained from eigenstates of many-body lattice Hamiltonians after tracing out part of the lattice. Two scenarios emerge for generic systems: (i) the diagonal entropy becomes equivalent to the thermodynamic entropy when a few sites are traced out (weak typicality); and (ii) the von Neumann (entanglement) entropy becomes equivalent to the thermodynamic entropy when a large fraction of the lattice is traced out (strong typicality). Remarkably, the results for few-body observables obtained with the reduced, diagonal, and canonical density matrices are very similar to each other, no matter which fraction of the lattice is traced out. Hence, for all physical quantities studied here, the results in the diagonal ensemble match the thermal predictions.

PACS numbers: 05.70.Ln, 05.30.-d, 05.45.Mt, 02.30.Ik

Despite advances, the emergence of thermodynamics from quantum mechanics is still a subject under debate. How to derive, from first principles, proper ensembles leading to the basic thermodynamic relations is not yet entirely clear. According to the concept of canonical typicality [1], the reduced density matrix of a subsystem of most pure states of many-particle systems is canonical. The proof of this statement requires a partition of the original system into a small “system” and a large “environment”. However, for example, suppose that our universe is in a pure state and that we trace out only a finite number of degrees of freedom. Can we describe the rest of the universe using statistical mechanics? How much one needs to trace out, how well the notion of canonical typicality works in finite systems, and which quantities will be more or less affected by the fraction of the original system traced out are questions that have received little attention. They are the more pressing given the progress made in experiments with ultracold gases [2].

We can discuss these issues in the context of entropy. If one takes an eigenstate of a generic many-body Hamiltonian and traces out the “environment” (\mathcal{E}), the grand canonical (GC) ensemble is the appropriate ensemble to describe the system (\mathcal{S}) that is left, where the total energy and number of particles fluctuate. One immediately realizes that the GC-entropy, S_{GC} , must be different from the von Neumann entropy, S_{vN} , if only a small fraction of the original system is traced out. In this case, S_{vN} is extensive in the size of the environment, instead of in the size of the system as S_{GC} . This follows from the fact that, for a composite system $\mathcal{S} + \mathcal{E}$ in a pure state $\hat{\rho} = |\Psi\rangle\langle\Psi|$, the reduced von Neumann entropy is defined as

$$S_{vN} \equiv -\text{Tr}_{\mathcal{S}} [\hat{\rho}_{\mathcal{S}} \ln \hat{\rho}_{\mathcal{S}}] \equiv -\text{Tr}_{\mathcal{E}} [\hat{\rho}_{\mathcal{E}} \ln \hat{\rho}_{\mathcal{E}}], \quad (1)$$

where the Boltzmann constant is set to unity and the reduced density matrix $\hat{\rho}_{\mathcal{S}} = \text{Tr}_{\mathcal{E}} \hat{\rho}$ and similarly $\hat{\rho}_{\mathcal{E}} = \text{Tr}_{\mathcal{S}} \hat{\rho}$. S_{vN} has been widely used to measure the entanglement in bipartite systems [3]. If the pure state is separable, $\hat{\rho} = \hat{\rho}_{\mathcal{S}} \otimes \hat{\rho}_{\mathcal{E}}$, then $S_{vN} = 0$, while maximum entanglement leads to $S_{vN} = \ln \mathcal{D}$, where \mathcal{D} is the smallest dimension of the two subsystems. The source of the disparity between S_{vN} and S_{GC} is the informa-

tion present in the off-diagonal elements of the reduced density matrix, which is not contained in the thermodynamic ensemble. When a large fraction of the original system is traced out, the equivalence between S_{vN} and S_{GC} is expected (canonical typicality). However, up to our knowledge, it has not been demonstrated for realistic systems.

Now suppose that instead of tracing out the environment, we physically cut it off and let the remaining system relax to equilibrium. We can then ask how much one needs to cut for the entropy of the reduced system to become equivalent to S_{GC} (if ever). After relaxation, this system is described by the diagonal ensemble [4, 5] obtained by writing the reduced density matrix ($\hat{\rho}_{\mathcal{S}}$) in the energy eigenbasis. The proper thermodynamic entropy in this case has been argued to be the diagonal entropy [6, 7], defined as

$$S_d \equiv - \sum_n \rho_{nn} \ln(\rho_{nn}), \quad (2)$$

where ρ_{nn} are the diagonal elements of the density matrix. S_d counts logarithmically the number of energy eigenstates which are occupied in \mathcal{S} . Unlike S_{vN} , S_d is extensive in the system size even if we trace a very small environment, e.g., a single degree of freedom. Cutting off the environment is equivalent to a sudden quench; it introduces to the system the (nonextensive) energy uncertainty $\delta E_{\mathcal{S}}$. This uncertainty implies that if all the eigenstates of the subsystem Hamiltonian $\hat{H}_{\mathcal{S}}$ within the window $\pm \delta E_{\mathcal{S}}$ are occupied with roughly the same weights, then $S_d \approx \log \Omega(E_{\mathcal{S}}) \delta E_{\mathcal{S}}$, where $\Omega(E_{\mathcal{S}})$ is the density of states in \mathcal{S} . Up to subextensive corrections, S_d would then coincide with the thermodynamic entropy of \mathcal{S} .

In this Letter, we study the properties of mixed states obtained from eigenstates of a many-body lattice Hamiltonian after tracing out or cutting off an increasingly large environment. One of our goals is to understand the structure of the remaining reduced density matrix and if it ever becomes thermal, which we monitor using S_{vN} , S_{GC} , and S_d . We find that, for nonintegrable systems, S_d approaches S_{GC} after cutting off a few (possibly one) sites, i.e., our hypothesis above is verified. S_{vN} , on the other hand, remains different from S_d

and S_{GC} until a large fraction of the lattice is traced out [8]. This motivates us to distinguish between the conventional (or strong) typicality $S_{vN} \cong S_d \cong S_{GC}$ and a weaker typicality in the sense that $S_{vN} \neq S_d \cong S_{GC}$. The latter implies that *only* the diagonal part of the density matrix of the reduced system in the energy eigenbasis exhibits a thermal structure.

Our results then show that the diagonal entropy satisfies the key thermodynamic relation:

$$\frac{\partial S_S}{\partial E_S} = \frac{\partial S_{\mathcal{E}}}{\partial E_{\mathcal{E}}} = \frac{1}{T}, \quad (3)$$

where E_S and $E_{\mathcal{E}}$ are the energies of the subsystems. This follows from the fact that S_d coincides with the thermodynamic entropy for S and \mathcal{E} simultaneously. In contrast, S_{vN} cannot satisfy this equality, as one can see by considering $\mathcal{E} \gg S$. In this case, $S_{vN} = S_S = S_{\mathcal{E}}$ is proportional to the size of S , while $E_{\mathcal{E}}$ is proportional to the size of \mathcal{E} , so $\partial S_{\mathcal{E}}/\partial E_{\mathcal{E}} \rightarrow 0$.

Another of our main goals in this work is to understand the description of few-body observables in the mixed states obtained by the two procedures mentioned before. For that, we study their expectation values as given by the reduced density matrix, the diagonal ensemble, and the GC ensemble. The results for the first two are similar even if very few sites are traced out and the system sizes are small. This suggests that either tracing out part of the original system or removing the same number of sites and waiting for the reduced system to relax leads to the same results, up to non-extensive boundary terms. For all practical purposes both procedures are then equivalent. The agreement with the GC expectation values is also good and improves with increasing system size. This implies that, for few-body observables, only weak typicality is needed to observe thermal behavior in experiments.

System.— We study hard-core bosons in a one-dimensional lattice with open-boundary conditions described by

$$\begin{aligned} \hat{H} = & \epsilon \left(\hat{n}_1 - \frac{1}{2} \right) \\ & + \sum_{i=1}^{L-1} \left[-t \left(\hat{b}_i^\dagger \hat{b}_{i+1} + \text{H.c.} \right) + V \left(\hat{n}_i - \frac{1}{2} \right) \left(\hat{n}_{i+1} - \frac{1}{2} \right) \right] \\ & + \sum_{i=1}^{L-2} \left[-t' \left(\hat{b}_i^\dagger \hat{b}_{i+2} + \text{H.c.} \right) + V' \left(\hat{n}_i - \frac{1}{2} \right) \left(\hat{n}_{i+2} - \frac{1}{2} \right) \right], \end{aligned} \quad (4)$$

where, t and t' [V and V'] are nearest-neighbor (NN) and next-nearest-neighbor (NNN) hopping [interaction], L is the chain size, and standard notation has been used [9]. Symmetries, and therefore degeneracies, are avoided by considering 1/3-filling and by placing an impurity ($\epsilon \neq 0$) on the first site. In what follows, $t = V = 1$ sets the energy scale, $\epsilon = 1/5$, and $t' = V'$. When $t' = V' = 0$, the model is integrable [10]. As the ratio between NNN and NN couplings increases, the system transitions to the chaotic domain [9].

For our calculations, we select an eigenstate $|\Psi_j\rangle$ of \hat{H} (4), with energy E_j closest to $E = \sum_j E_j e^{-E_j/T} / \sum_j e^{-E_j/T}$ corresponding to an effective temperature T . We then trace

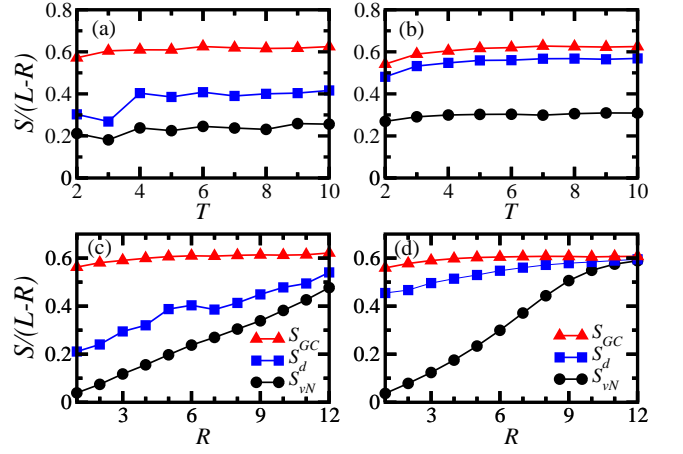


FIG. 1: (Color online) (a),(b) Entropies per site vs temperature for $R = L/3$. (c),(d) Entropies per site vs R for a fixed temperature; $T = 4$. (a),(c) $t' = V' = 0$ (integrable); (b),(d) $t' = V' = 0.32$ (chaotic). All panels: $L = 18$.

out a certain number of sites $R \leq 2L/3$, on the right side of the chain, and study the entropies and observables of the reduced system. The reduced density matrix $\hat{\rho}_S$ describing the remaining system consists of different subspaces each with a number $N \in [\max(L/3 - R, 0), L/3]$ of particles.

Entropies.— The von Neumann, diagonal, and GC entropies are given by Eq. (1), Eq. (2), and

$$S_{GC} = \ln \Xi + \frac{E_S - \mu N_S}{T_{GC}}, \quad (5)$$

respectively. In Eq. (5), $\Xi = \sum_n e^{(\mu N_n - E_n)/T_{GC}}$ is the grand partition function, T_{GC} is the GC temperature, μ is the chemical potential, and $E_S = \text{Tr}[\hat{H}_S \hat{\rho}_S]$ and $N_S = \text{Tr}[\hat{N}_S \hat{\rho}_S]$ are, respectively, the average energy and number of particles in the remaining subsystem S .

Results.— In Fig. 1, we show results for S_{vN} , S_d , and S_{GC} in the integrable [(a),(c)] and chaotic [(b),(d)] domains. Larger fluctuations are seen in Figs. 1(a) and 1(c) as characteristic of the integrable regime. Figs. 1(a) and 1(b) show the entropies vs different eigenstates, which are increasingly away from the ground state (T increases), when 1/3 of the sites are traced out. In the chaotic regime, and for all states selected, one can see that S_d is close to S_{GC} , while S_{vN} is quite far. This is remarkable as it hints a thermal structure in the diagonal part of the reduced density matrix in the energy eigenbasis.

In Figs. 1(c) and 1(d) we show results for a fixed T as an increasingly larger fraction of the original system is traced out. One can see again that in the chaotic limit S_d is much closer to S_{GC} than to S_{vN} , even when very few sites are traced out. However, in both regimes, all entropies approach each other as the fraction of sites traced out increases. For the lattice sizes considered here, we need to trace out more than one half of the chain for the effects of the off-diagonal elements of the density matrix to become irrelevant in S_{vN} , leading this entropy to finally approach S_d and S_{GC} .

The results presented in Fig. 1 were obtained for $L = 18$,

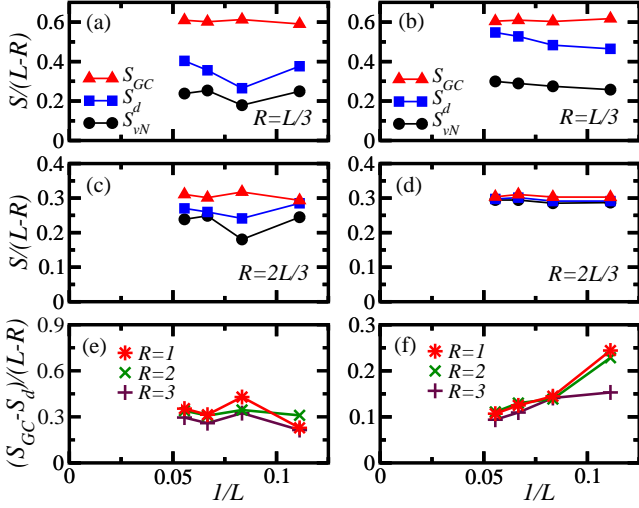


FIG. 2: (Color online) (a)–(d) Entropies per site vs $1/L$ for $T = 4$ and a fixed ratio R/L (indicated). (e), (f) $S_{GC} - S_d$ per site vs $1/L$ for $R = 1, 2$, and 3 . (a), (c), (e) $t' = V' = 0$ (integrable); (b), (d), (f) $t' = V' = 0.32$ (chaotic).

the largest system size that we can study with full exact diagonalization. Figure 2 depicts the scaling of the entropies in both domains, integrable [(a), (c)] and nonintegrable [(b), (d)], and for $T = 4$. In Figs. 2(a) and 2(b), when $L/3$ sites are cut off, S_d and S_{GC} approach each other as L increases, up to a possible non-extensive correction. This trend is seen for all systems we have studied in the chaotic regime [13], and opens up a new question: could cutting off an infinitesimal part of the original system lead S_d and S_{GC} to be equal in the thermodynamic limit? In Figs. 2(e) and 2(f), we show the difference between S_{GC} and S_d per site vs system size when tracing out one, two, or three sites. In the chaotic regime [Fig. 2(f)], the results are consistent with a vanishing difference in the thermodynamic limit (even when cutting one site [13]). Hence, one could argue that single eigenstates of many-body Hamiltonians have a thermodynamic entropy [8]. Close to the integrable point [Figs. 2(a), 2(c), and 2(e)], large fluctuations are observed for different values of T and t', V' , which makes it difficult to draw general conclusions.

In Figs. 2(a) and 2(b), one can also see that for $R = L/3$, the von Neumann entropy (per site) saturates to a different value from S_d and S_{GC} (per site), as the lattice size increases. As shown in Figs. 2(c) and 2(d), it is only when $R > L/2$ that the three entropies become comparable. However, for our system sizes, this happens only in the chaotic regime. As one approaches the integrable point, we again find large fluctuations and the results depend on T and the values of t', V' . Fluctuations in the integrable regime are understandable. In the chaotic regime (and away from the edges of the spectrum) all eigenstates of the Hamiltonian that are close in energy have (i) a similar structure, as reflected by the inverse participation ratio and information entropy in different bases [9], and (ii) thermal expectation values of few-body observables [4, 5, 14, 15]. However, this is not the case close to integrability where most

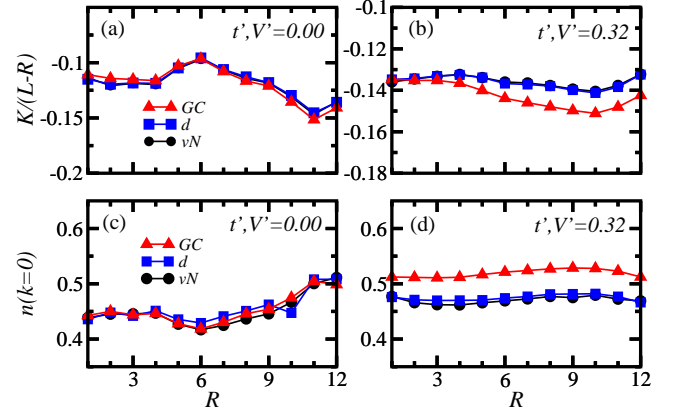


FIG. 3: (Color online) (a), (b) Kinetic energy per site and (c), (d) $n(k=0)$ vs R ; $L = 18$; $T = 4$. (a), (c) $t' = V' = 0$ (integrable); (b), (d) $t' = V' = 0.32$ (chaotic).

quantities fluctuate wildly between eigenstates close in energy [4, 5, 9, 15], and this is affecting our results here.

Observables.—An important question we are left to address is whether the extra information carried by the off-diagonal elements of the reduced density matrix is of relevance to quantities measured experimentally. We focus our analysis on few-body observables. Their expectation values from the reduced, diagonal, and grand canonical density matrices are given by

$$O_{vN} = \text{Tr}[\hat{O}\hat{\rho}_S], \quad O_d = \sum_n \rho_{nn} O_{nn}, \quad (6)$$

$$O_{GC} = \frac{1}{\Xi} \sum_n O_{nn} e^{(\mu N_n - E_n)/T}, \quad (7)$$

respectively. Here, $O_{nn} = \langle \psi_n | \hat{O} | \psi_n \rangle$ and $|\psi_n\rangle$'s are the eigenstates of the Hamiltonian in the reduced system.

Results.—Figure 3 shows results for the kinetic energy

$$\hat{K} = -t \sum_{i=1}^{L-R-1} (\hat{b}_i^\dagger \hat{b}_{i+1} + \text{H.c.}) - t' \sum_{i=1}^{L-R-2} (\hat{b}_i^\dagger \hat{b}_{i+2} + \text{H.c.}), \quad (8)$$

and the momentum distribution function,

$$\hat{n}(k) = \frac{1}{L-R} \sum_{j,l=1}^{L-R} e^{i \frac{2\pi k}{L-R} (j-l)} \hat{b}_j^\dagger \hat{b}_l, \quad (9)$$

for an increasingly large fraction of sites traced out. The results obtained with the three density matrices are comparable, independently of the regime, the number of sites traced out, and T (see [13]). In particular, the fact that O_{vN} and O_d are so close demonstrates that both procedures, tracing sites out or cutting off part of the original system and then measuring the observables after relaxation, lead to similar outcome. The information contained in the off-diagonal elements of the reduced density matrix, which generates discrepancies between S_{vN} and $S_d \cong S_{CG}$, is therefore irrelevant to few-body observables. Our findings also open the interesting question:

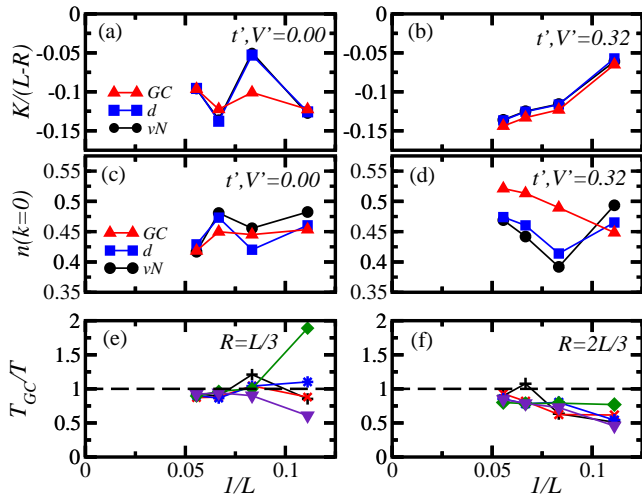


FIG. 4: (Color online) (a)–(d) Observables vs $1/L$ for $R = L/3$. (e),(f) Ratio between the grand-canonical temperature and the temperature vs $1/L$. (Black) Plus: $t' = V' = 0.04$; (red) cross: $t' = V' = 0.08$; (blue) star: $t' = V' = 0.16$; (green) diamond: $t' = V' = 0.32$; (purple) down-triangle: $t' = V' = 0.64$. In all panels: $T = 4$.

which experimentally measurable quantities (if any) could distinguish between tracing sites out or cutting them off?

We note that, in the chaotic regime, the GC results for both observables depart from those obtained with the reduced and diagonal density matrices as R increases. This is understandable because the GC results are obtained for a system with $L - R$ sites and open boundary conditions, while the other two are obtained for a system with L sites from which R sites are either traced out or cut off. Hence, the more sites one cuts off (the larger the value of R), the smaller is the system remaining. Finite size effects are then expected to be stronger, in particular as the values of t', V' increase. It is also expected that they should vanish in the thermodynamic limit.

In Figs. 4(a)–4(d), we show the scaling behavior of the two observables from Fig. 3 for $R = L/3$. It is apparent that, in the chaotic regime [Figs. 4(b) and 4(d)], the observables calculated in the three ensembles approach each other with increasing system size. (Results for other temperatures and observables in the chaotic domain are presented in Ref. [13]). In the integrable limit [Figs. 4(a) and 4(c)], large fluctuations prevent us from reaching general conclusions. This is a regime that needs to be studied by other means, which may allow one to do a proper extrapolation to the thermodynamic limit.

A final remarkable property of the mixed states studied here is that their effective thermodynamic temperature (T_{GC}) is the same as the effective temperature T of the many-body eigenstate from which they are obtained. This is shown in Figs. 4(e) and 4(f), where we plot T_{GC}/T vs $1/L$ for $R = L/3$ [4(e)] and $R = 2L/3$ [4(f)], and for different values of t', V' . The two temperatures are close (except for the smallest systems sizes) and further approach each other as $1/L$ decreases, which is consistent with the idea of eigenstate thermalization where a single eigenstate exhibits thermal behavior [4, 14].

Conclusions.— We have found that, away from integrability, the diagonal and grand canonical entropies are very close to each other, even when a small portion (probably an infinitesimal fraction) of the lattice is cut off. They further approach each other with increasing system size. In contrast to S_d , S_{vN} only approaches S_{GC} when a large part of the original system is traced out. This behavior reflects the non-diagonal structure of the reduced density matrix when only small fractions of the lattice are traced out. Led by these results, we identified two different regimes: weak typicality, where the diagonal ensemble develops a thermal structure, and strong (canonical) typicality, where the density matrix of the reduced system is thermal. Close to and at integrability further studies are necessary. Our results exhibit large fluctuations depending on the state selected and the values of t', V' .

We also studied experimentally measurable few-body observables as determined from the reduced, diagonal, and grand-canonical density matrices. We find that they all lead to the same results as the system size increases, no matter how many sites are traced out. This demonstrates that the extra information contained in the off-diagonal elements of the reduced density matrix is irrelevant to those observables. Therefore, it is plausible to conjecture that the expectation values of *physical* observables in subsystems of any size obtained from generic many-body eigenstates can be entirely obtained from standard statistical ensembles. Our results show that even in relatively small systems, both procedures, tracing out the “bath” or cutting it off and letting the subsystem thermalize, lead to the same outcome.

This work was supported by the NSF under grant DMR-1147430 (L.F.S.), the Office of Naval Research (M.R.), the NSF under grant DMR-0907039, the AFOSR under grant FA9550-10-1-0110, and the Sloan Foundation (A.P.). We thank J. Deutsch for useful discussions.

Note added.— After completion of this work, we have learned that the strong (canonical) typicality has been recently verified in translationally invariant systems [16].

-
- [1] H. Tasaki, Phys. Rev. Lett. **80**, 1373 (1998); S. Popescu, A. J. Short, and A. Winter, Nature Phys. **2**, 754 (2006); S. Goldstein, J. L. Lebowitz, R. Tumulka, and N. Zanghì, Phys. Rev. Lett. **96**, 050403 (2006).
 - [2] M. Greiner, O. Mandel, T. W. Hansch, and I. Bloch, Nature **419**, 51 (2002); T. Kinoshita, T. Wenger, and D. S. Weiss, Nature **440**, 900 (2006); S. Hofferberth *et al.*, Nature **449**, 324 (2007); S. Trotzky *et al.*, arXiv:1101.2659.
 - [3] C. Mejia-Monasterio, G. Benenti, G. Carlo, and G. Casati, Phys. Rev. A **71**, 062324 (2005); L. Amico, R. Fazio, A. Osterloh, and V. Vedral, Rev. Mod. Phys. **80**, 517 (2008).
 - [4] M. Rigol, V. Dunjko, and M. Olshanii, Nature **452**, 854 (2008).
 - [5] M. Rigol, Phys. Rev. Lett. **103**, 100403 (2009); Phys. Rev. A **80**, 053607 (2009).
 - [6] A. Polkovnikov, Ann. Phys. (N.Y.) **326**, 486 (2011).
 - [7] L. F. Santos, A. Polkovnikov, and M. Rigol, Phys. Rev. Lett. **107**, 040601 (2011).

- [8] J. M. Deutsch, New J. Phys. **12**, 075021 (2010).
 [9] L. F. Santos and M. Rigol, Phys. Rev. E **81**, 036206 (2010); Phys. Rev. E **82**, 031130 (2010).
 [10] This system can be mapped onto a spin-1/2 chain [11]. In the presence of NN couplings only, the spin-1/2 model remains integrable even after the addition of a local impurity field on the edge of the chain [12].
 [11] T. Holstein and H. Primakoff, Phys. Rev. **58**, 1098 (1940).

- [12] F. C. Alcaraz, M. N. Barber, M. T. Batchelor, R. J. Baxter, and G. R. W. Quispel, J. Phys. A **20**, 6397 (1987).
 [13] See supplementary material.
 [14] J. M. Deutsch, Phys. Rev. A **43**, 2046 (1991); M. Srednicki, Phys. Rev. E **50**, 888 (1994).
 [15] C. Neuenhahn and F. Marquardt, arXiv:1007.5306 (2010).
 [16] J. M. Deutsch, H. Li, and A. Sharma, arXiv:1202.2403.

Supplementary material for EPAPS Weak and strong typicality in quantum systems

Lea F. Santos¹, Anatoli Polkovnikov², and Marcos Rigol³

¹Department of Physics, Yeshiva University, New York, NY 10016, USA

²Department of Physics, Boston University, Boston, MA 02215, USA

³Department of Physics, Georgetown University, Washington, DC 20057, USA

ENTROPIES

Figure 5 provides further support to our statement that S_d approaches S_{GC} as the system size increases. This fact holds even for the smallest value $R = 1$, suggesting that in the thermodynamic limit, the diagonal density matrix becomes a thermal density matrix when an infinitesimally small part of the system is traced out.

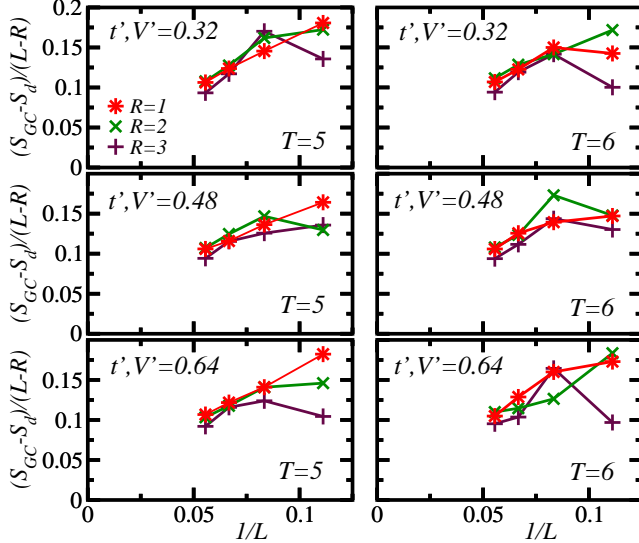


FIG. 5: (Color online) $S_{GC} - S_d$ per site vs $1/L$ for the three smallest values of R . The values of t', V' are indicated and they imply chaoticity.

OBSERVABLES

Figure 6 reinforces that the expectation values of few-body observables obtained with the reduced, diagonal, and grand canonical density matrices are comparable, independently of

the regime, the number of sites traced out, and T . In the figure we show the behavior of physical observables vs temperature. We consider the kinetic energy, the momentum distribution function for $k = 0$ and $k = 1$, and the interaction energy:

$$\hat{I} = V \sum_{i=1}^{L-R-1} \left(\hat{n}_i^b - \frac{1}{2} \right) \left(\hat{n}_{i+1}^b - \frac{1}{2} \right) \quad (10)$$

$$+ V' \sum_{i=1}^{L-R-2} \left(\hat{n}_i^b - \frac{1}{2} \right) \left(\hat{n}_{i+2}^b - \frac{1}{2} \right).$$

The results for O_d and O_{vN} are very similar throughout. They indicate that the information contained in the off-diagonal elements of the reduced density matrix is therefore irrelevant to few-body observables. We note that while O_{GC} is also very close to O_d and O_{vN} , the GC results for $n(k=0)$ and I are slightly more separated, since these observables are more sensitive to finite size and boundary effects than K .

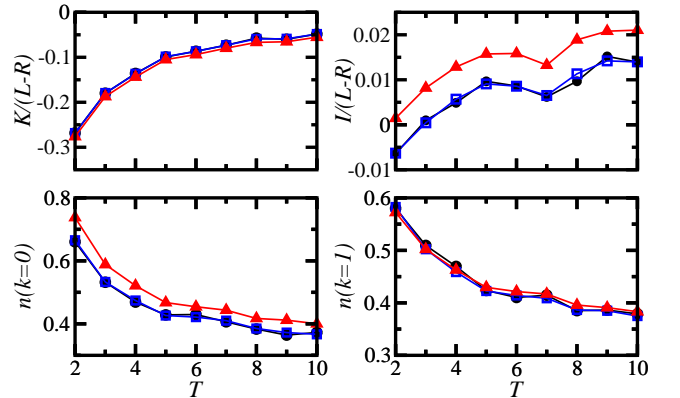


FIG. 6: (Color online) Interaction energy per site, kinetic energy per site, and momentum distribution function for $k = 0$ and $k = 1$ vs temperature; $L = 18$; $R = L/3$; $t' = V' = 0.32$. Triangles: O_{GC} , squares: O_d , and circles: O_{vN} .

The scaling behavior of the observables considered here are shown in Fig. 7 for $R = L/3$ and values of t', V' in the chaotic region. In this regime, the observables calculated in the three ensembles approach each other with increasing system size.

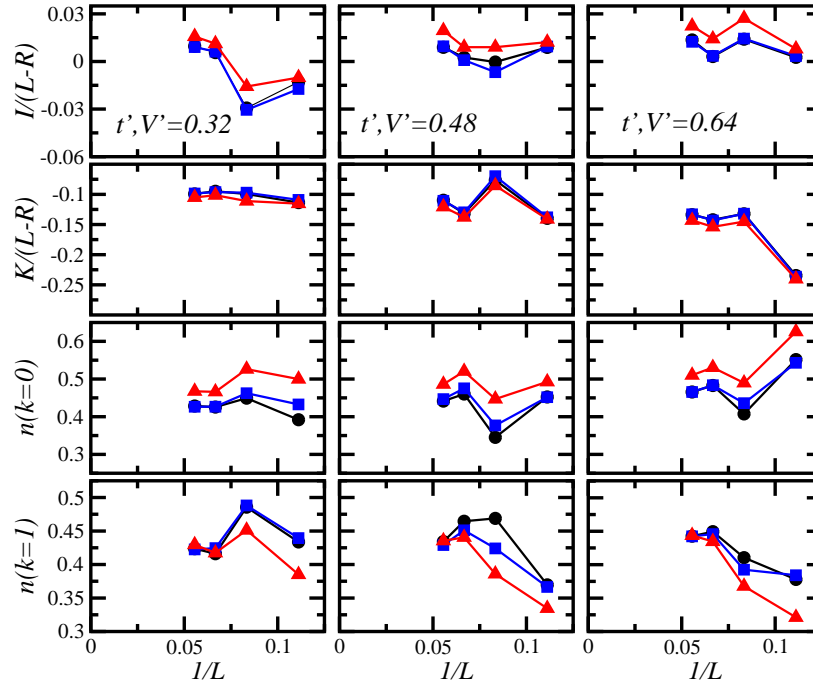


FIG. 7: (Color online) Interaction energy per site, kinetic energy per site, and momentum distribution function for $k = 0$ and $k = 1$ vs $1/L$; $T = 5$. Triangles: O_{GC} , squares: O_d , and circles: O_{vN} ; $R = L/3$. The values of t', V' for each column are indicated at the top panels.